Water Research X 27 (2025) 100294

Contents lists available at ScienceDirect

Water Research X

journal homepage: www.sciencedirect.com/journal/water-research-x

Emerging and legacy organophosphate flame retardants in the tropical estuarine food web: Do they exhibit similar bioaccumulation patterns, trophic partitioning and dietary exposure?

Qianyi Huang [a,g], Rui Hou [b,*], Yuchen Wang [d], Lang Lin [e], Hengxiang Li [a], Shan Liu [a], Xiangrong Xu [c,*], Kefu Yu [c,f], Xiaoping Huang [a]

[a] Key Laboratory of Tropical Marine Bio-resources and Ecology, Guangdong Provincial Key Laboratory of Applied Marine Biology, South China Sea Institute of Oceanology, Chinese Academy of Sciences, Guangzhou 510301, China
[b] Guangdong Provincial Key Laboratory of Water Quality Improvement and Ecological Restoration for Watersheds, School of Ecology, Environment and Resources, Guangdong University of Technology, Guangzhou 510006, China
[c] Guangxi Laboratory on the Study of Coral Reefs in the South China Sea, Coral Reef Research Center of China, School of Marine Sciences, Guangxi University, Nanning 530004, China
[d] College of Life Sciences and Engineering, Jinan University, Guangzhou 510632, China
[e] South China Sea Bureau of Ministry of Natural Resources, Guangzhou 510310, China
[f] Southern Marine Science and Engineering Guangdong Laboratory (Guangzhou), Guangzhou 511458, China
[g] University of Chinese Academy of Sciences, Beijing 100049, China

ARTICLE INFO

Keywords:
Legacy and emerging organophosphate flame retardants
Bioaccumulation
Trophic transfer
Organism partitioning
Biotransformation

ABSTRACT

Emerging organophosphate flame retardants (E-OPFRs) are a new class of pollutants that have attracted increasing attention, but their bioaccumulation patterns and trophodynamic behaviors in aquatic food webs still need to be validated by comparison with legacy OPFRs (L-OPFRs). In this study, we simultaneously investigated the bioaccumulation, trophic transfer, and dietary exposure of 8 E-OPFRs and 10 L-OPFRs in a tropical estuarine food web from Hainan Island, China. Notably, the Σ_{10}L-OPFRs concentration (16.1–1.18 × 10^5 lipid weight (lw)) was significantly greater than that of Σ_8E-OPFRs (nondetectable (nd) - 2.82 × 10^3 ng/g lw) among the investigated organisms, and they both exhibited similar trends: fish<mollusk<crustacean. Significant biomagnification was found only for triphenyl phosphate (TPHP, an L-OPFR) with a trophic magnification factor (TMF) of 1.55, whereas other E- and L-OPFRs showed limited trophic transfer potential. Storage lipid was the dominant adsorption phase for most E-OPFRs and L-OPFRs on the basis of the fugacity approach. The water content controls the main trophic partitioning for the L-OPFRs of triethyl phosphate (TEP) and tris(2-chloroethyl) phosphate (TCEP) in the food web. Storage lipid and structure protein are equally important for 2,2-bis(chloromethyl)-propane-1,3-diyltetrakis(2-chloroethyl) biphosphate (V6, an emerging OPFR). The investigation of metabolites and the biotransformation rate (K_M) confirmed the role of biotransformation in offsetting trophic transfer for both legacy and emerging OPFRs. Furthermore, the hazard quotients (HQs) were found to be <1 for South China residents for both the E- and L-OPFRs, but the health risks of these two kinds of OPFRs should be given sustained attention.

1. Introduction

Organophosphate flame retardants (OPFRs) have been commonly used as chemicals to increase the flame retardancy of various materials for decades, such as plastics, rubber, textiles, and electronic equipment (Du et al., 2019; Hou et al., 2016). The prohibition and restriction of the use of legacy OPFRs (L-OPFRs), such as TCEP, tris(1,3-dichloro-2-propyl) phosphate (TDCPP) and tri(chloro-2-propyl) phosphate (TCPP), in children's products, furniture, mattresses, and electronics have been pronounced by the US, Canada and the EU (Blum et al., 2019; Pantelaki and Voutsa, 2019; van der Veen and de Boer, 2012), and TCEP is also listed in the "Second batch of priority controlled

* Corresponding authors.
E-mail addresses: ruihou@gdut.edu.cn (R. Hou), xuxr@gxu.edu.cn (X. Xu).

https://doi.org/10.1016/j.wroa.2024.100294
Received 19 October 2024; Received in revised form 20 November 2024; Accepted 9 December 2024
Available online 10 December 2024

chemicals list" in China (China MEE, 2020). In recent years, a growing number of nonhalogenated emerging OPFRs (E-OPFRs), such as diphenyl p-tolyl phosphate (CDP), 8-methylnonyl diphenyl phosphate (iDDPHP), and tris(4-tert-butylphenyl) phosphate (T4tBPP), have been introduced as substitutes for legacy OPFRs. The global OPFR market size was approximately ¥ 5.4 billion in 2022 and is expected to reach ¥ 7.9 billion in 2029 on the basis of QYResearch (2023).

Compared with legacy OPFRs, emerging OPFRs generally have higher molecular weights, longer half-lives and greater hydrophobicity (Luo et al., 2023; Ye et al., 2023). Notably, some emerging OPFRs exhibit comparable or even greater toxic effects than legacy OPFRs. For example, the effects of tris(4-isopropylphenyl) phosphate (iPPP) were greater than those of L-OPFRs (TPHP, tricresyl phosphate (TCP) and 2-ethylhexyl diphenyl phosphate (EHDPHP)) on mitochondrial activity, oxidative stress, and steroid secretion in mouse Leydig tumor cells (Schang et al., 2016), and energy metabolism was found to be more effectively inhibited by CDP than by L-OPFRs such as TPHP, TCEP, TDCPP, tris(2-ethylhexyl) phosphate (TEHP), tris(2-butoxyethyl) phosphate (TBOEP), and tris-n-butyl phosphate (TNBP) (Tsugoshi et al., 2020). In addition, emerging OPFRs have been detected in many aquatic environments, such as the Yangtze River Basin (Li et al., 2023), Taihu Lake (Ye et al., 2022; Zhao et al., 2019), and Laizhou Bay (Bekele et al., 2019). The effects on aquatic organisms and the potential risk of E-OPFRs have recently attracted widespread attention from scholars in the water environment field (Shi and Zhao, 2024; Xie et al., 2024b).

The extensive and widespread distribution of emerging OPFRs inevitably leads to increased exposure to aquatic animals (Shi and Zhao, 2024). Significantly increased E-OPFRs accumulation was detected in marine mammals (cetaceans and finless porpoises) from 2007 to 2020 (Xie et al., 2024a, 2024b). Previous studies have suggested that partitioning and biotransformation are the most important factors in the determination of bioaccumulation and trophic transfer of nonpersistent compounds in aquatic food webs (Huang et al., 2023; Kim et al., 2002). Compared with the commonly used Log K_{OW}, the organism-water partition coefficient ($K_{organism\text{-}water}$) is a more suitable descriptor for predicting bioaccumulation potential because of its partitioning in different tissue compartments (i.e., lipid, phospholipid, protein, and water) (Endo and Goss, 2014; Geisler et al., 2012; Huang et al., 2023). In addition, the estimated inherent K_M values and metabolite accumulation can provide insight into the biotransformation of OPFRs to characterize their compound-specific trophodynamics. Joint partitioning and biotransformation efforts can offer an opportunity to yield new insights into the bioaccumulation and trophic transfer mechanisms of E- and L-OPFRs in aquatic food webs.

To the best of our knowledge, whether the bioaccumulation potential and trophic transfer behavior of E-OPFRs are similar to those of legacy analogs in aquatic food webs remain unclear. For example, CDP showed trophic dilution in aquatic food webs for wild fish in Poyang Lake but exhibited significant trophic magnification potential in the marine food web of Laizhou Bay (Bekele et al., 2019; Yan et al., 2024). Bisphenol A bis (diphenyl phosphate) (BDP) was significantly biodiluted in Laizhou Bay, whereas no such trend was observed in Taihu Lake (Lian et al., 2024; Zhao et al., 2019). It is imperative to conduct pertinent studies without elucidation of the bioaccumulation and trophic transfer mechanisms involved. Hainan Island, China, is a region with distinctive characteristics, with relatively high levels of OPFRs pollution originating from both local and surrounding cities/countries (Mo et al., 2019). Therefore, the estuary (Nandu River Estuary) can be considered the ideal area to clarify the bioaccumulation pattern, the fugacity- and biotransformation-based mechanisms of trophic transfer, and the potential health risks of legacy and emerging OPFRs in the aquatic food web. The objectives of this study were to 1) compare the occurrence and accumulation of selected 8 emerging and 10 legacy OPFRs in marine environments and organisms; 2) characterize the different trophic partitioning of these OPFRs and introduce $K_{organism\text{-}water}$ and metabolite-quantified to clarify the primary influencing mechanisms; and 3) assess and compare the potential health risks of legacy and emerging OPFRs from seafood.

2. Results and discussion

2.1. Bioaccumulation of emerging and legacy OPFRs in the tropical estuarine food web

The concentrations of the 8 emerging and 10 legacy OPFRs in seawater and sediments from the Nandu River Estuary are provided in Fig. 1-A, B, Tables 1 and 2. Tris(2,4-di-tert-butylphenyl) phosphate (TDtBPP) (309±108 ng/L), iPPP (0.077±0.111 ng/L) and V6 (0.067 ±0.114 ng/L) are the most abundant E-OPFRs in seawater. TDtBPP was also the predominant E-OPFRs in the sediment samples (350±283 ng/g dw), which is not only produced industrially but also susceptible to the oxidation of tris(2,4-di-*tert*-butylphenyl) phosphite (AO168), leading to its high abundance in the environment (Gao et al., 2024; Liu and Mabury, 2018; Zhou et al., 2024). EHDPHP and TEHP are the most abundant legacy OPFRs in seawater, whereas TEP and TDCPP are dominant in sediment. Compared with those of the 10 legacy OPFRs, the total concentrations of the 8 emerging OPFRs were relatively greater in both seawater (309±109 ng/L) and sediments (350±283 ng/g dw).

In the food web samples, the mean total concentrations of Σ_{10}L-OPFRs and Σ_8E-OPFRs both showed an increasing trend among species: fish ($775 \pm 1.53 \times 10^3$ and 137 ± 209 ng/g lw) < mollusk ($1.60 \times 10^4 \pm 3.21 \times 10^4$ and 160 ± 246 ng/g lw) < crustacean ($4.63 \times 10^4 \pm 4.03 \times 10^4$ and 464 ± 881 ng/g lw), respectively (Fig. 1-A, Tables 1 and 2). (3-diphenoxyphosphoryloxyphenyl) diphenyl phosphate (RDP), iDDPHP and TDtBPP were the most accumulated emerging OPFRs, with average concentrations of 120 ng/g lw, 29.9 ng/g lw and 21.1 ng/g lw, respectively, whereas TDCPP (10,913 ng/g lw), TBOEP (259 ng/g lw), TCPP (89.9 ng/g lw), TCP (87.3 ng/g lw) and TPHP (70.7 ng/g lw) were important legacy OPFRs (Fig. 1-B). The average concentrations of the other emerging OPFRs were lower than 10.8 ng/g lw. A weak correlation of the total concentration was found between L- and E-OPFRs, which suggested that they may exhibit different environmental behaviors or sources (Figure S1). The concentrations of RDP and iDDPHP in the biota were higher than those in the water and sediment, which may be attributed to the moderate Log K_{OW} values of RDP (5.97) and iDDPHP (5.44) for bioaccumulation (Arnot and Gobas, 2006). Among legacy OPFRs, TDCPP and TCPP are well documented as important OPFR congeners in aquatic organisms because of their ubiquitous distribution and persistence in the environment (Choi et al., 2020; Fu et al., 2021; Xie et al., 2024b; Yan et al., 2024). Principal component analysis (PCA) revealed no distinct differences in the OPFRs distributions between the environmental matrices and biota or between the emerging and legacy OPFRs (Figure S2).

The log BAF value is usually employed as a metric to assess the bioaccumulation potential, where a value lower than 3.3 (wet weight-based, criterion B in Annex XIII of REACH) indicates a low bioaccumulation effect for the investigated chemicals. The log BAFs for the emerging OPFRs were in the range of −1.33–1.44, except for CDP, RDP and BDP (nd in seawater) (Fig. 1-C, Table S1). All legacy OPFRs had log BAF values ranging from −2.27–1.75 for all species (Fig. 1-C, Table S2). Overall, the studied emerging and legacy OPFRs have a limited bioaccumulation capacity in the investigated food web. The mean BSAF values of legacy and emerging OPFRs ranged from 0.004 to 27.4 and from 0.003 to 158, respectively (Tables S1 and S2). Among them, legacy OPFRs of TDCPP, TPHP, TBOEP, TCP and TEHP and emerging OPFRs of CDP, RDP, iDDPHP, iPPP and T4tBPP in some species were higher than 1, indicating that these compounds tend to accumulate in specific species rather than in sediment. In comparison, E-OPFRs have relatively high bioaccumulation potentials in the food web, and water uptake might be the main exposure route of most OPFRs in organisms.

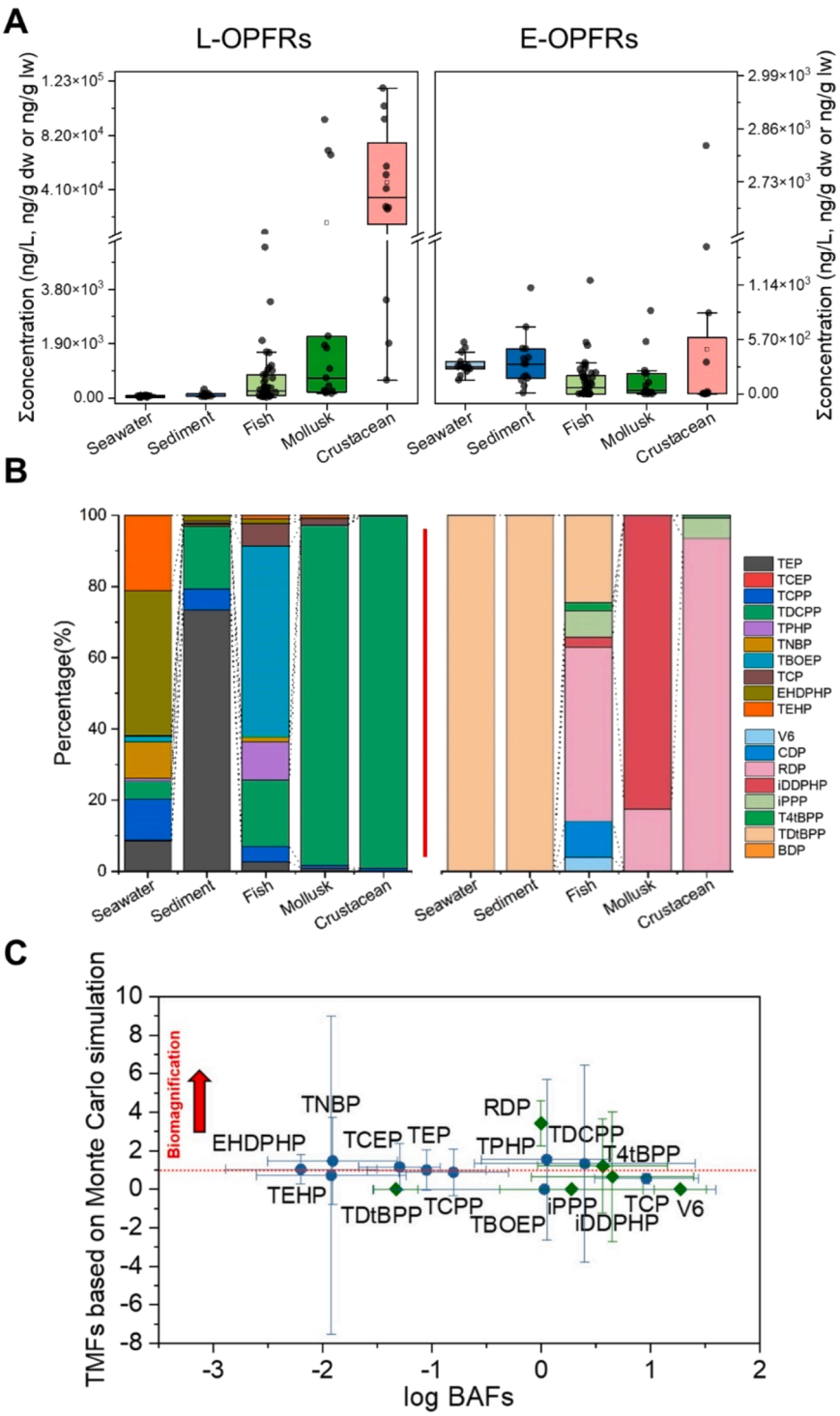

Fig. 1. Bioaccumulation of legacy and emerging OPFRs in the environment matrices and estuarine biotas from the Nandu River Estuary. (A) Total legacy and emerging OPFR concentrations, (B) legacy and emerging OPFR profiles, and (C) comparison of the log bioaccumulation factors (log BAFs) with the trophic magnification factor (TMF). The threshold values were set for bioaccumulation (log BAFs > 3.30) and biomagnification (TMF > 1). All the factor values are presented as the means ± standard deviations.

2.2. Trophodynamic differences between emerging and legacy OPFRs

The $\delta^{13}C$ and $\delta^{15}N$ values ranged from −23.8 ‰ to −14.7 ‰ and 3.44 ‰ to 15.8 ‰, respectively, in the food web (Figure S3-A and Table S3). A statistically significant correlation was observed between the $\delta^{13}C$ and $\delta^{15}N$ values ($r^2 = 0.4944$, $p < 0.001$), indicating analogous marine habitats for these species. The relative trophic levels (TLs) of the observed organisms ranged from 1.13 to 4.67 (Figure S3-B and Table S3). To reduce uncertainty, only OPFRs with detection frequency (DF) >30.0 % in the organisms were used to calculate the TMFs (Tables S1 and S2). The TMFs of TPHP, TCP and iDDPHP estimated by the slope of the concentration-TL relationship (TMF_{OLS}) were 1.55, 0.514 and 0.505, respectively ($p < 0.05$). In addition, TEHP showed a marginally significant relationship with TLs ($p = 0.05$, TMFs = 0.519; Fig. 2) in this study, indicating that TEHP tends to biodilute in this food web. The log-transformed concentrations of other legacy OPFRs (TCEP,

Table 1
Details on the concentrations of 8 emerging OPFRs in seawater (ng/L, $n = 14$), sediment (ng/g dw, $n = 14$), and biological samples (ng/g lipid weight).

Categories	Species name	V6	CDP	RDP	iDDPHP	BDP	iPPP	T4tBPP	TDtBPP	Σ_8E-OPFRs
Seawater	Dissolved phase	nd	nd	nd	nd	nd	nd	nd	178±95.7	178±95.7
	Detection frequency (%)	0.000	0.000	0.000	0.000	0.000	0.000	0.000	100	100
	Particulate phase	0.067 ±0.114	nd	nd	0.018 ±0.017	nd	0.077 ±0.111	0.010 ±0.019	131±64.2	131±64.1
	Detection frequency (%)	28.6	0.000	0.000	57.1	0.000	42.9	50.0	100	100
	Total	0.067 ±0.114	nd	nd	0.018 ±0.017	nd	0.077 ±0.111	0.010 ±0.019	309±108	309±109
	Detection frequency (%)	28.6	0.000	0.000	57.1	0.000	42.9	50.0	100	100
Sediment		0.077 ±0.198	0.004 ±0.012	0.020 ±0.075	0.022 ±0.026	nd	0.053 ±0.136	0.004 ±0.009	350±283	350±283
	Detection frequency (%)	14.3	14.3	7.14	50	0.000	14.3	14.3	100	100
Fish	*Epinephelus fasciatus*	nd	17.5 ± 30.3	108±57.4	2.26±3.91	nd	7.45±12.9	13.8 ± 12.7	344±596	493±598
	Chorinemus formosanus	nd	68.9 ± 119	nd	1.93±3.34	nd	nd	2.16±1.34	nd	73.0 ± 124
	Acanthopagrus latus	nd	nd	nd	0.503 ±0.524	nd	0.882 ±0.578	<MDL	108±188	110±187
	Terapon jarbua	nd	nd	nd	0.728 ±0.733	nd	0.556 ±0.963	1.08±1.23	nd	2.36±1.81
	Siganus canaliculatus	nd	42.2 ± 47.7	90.0 ± 85.2	2.84±2.70	nd	2.39±4.14	nd	nd	137±117
	Sillago sihama	38.1 ± 65.9	nd	nd	0.139 ±0.241	nd	nd	nd	nd	38.2 ± 65.8
	Leiognathus brevirostris	nd	nd	247±65.8	6.00±1.18	nd	77.5 ± 134	8.08±7.53	nd	338±183
	Pneumatophorus japonicus	43.2 ± 74.8	nd	35.2 ± 60.9	4.48±2.52	nd	26.6 ± 46.0	1.71±1.70	nd	111±108
	Gnathanodon speciosus	nd	59.2 ± 88.7	nd	2.56±1.25	nd	20.2 ± 27.6	0.494 ±0.856	nd	82.5 ± 117
	Plectorhinchus	nd	nd	nd	23.1 ± 38.6	nd	0.455 ±0.788	0.190 ±0.329	nd	23.8 ± 38.1
	Stolephorus chinensis	nd	18.7 ± 32.3	287±139	0.679 ±0.605	nd	2.38±4.13	0.946 ±0.839	nd	310±174
	Trachinotus ovatus	nd	nd	77.8 ± 87.4	0.874 ±0.757	nd	0.212 ±0.367	2.31±4.00	53.3 ± 92.4	135±62.6
	Pisodonophis boro	nd	nd	nd	2.00±1.77	nd	4.75±7.45	nd	nd	6.75±8.67
	Lutjanus johni	nd	nd	nd	<MDL	nd	<MDL	<MDL	nd	0.085 ±0.060
	Trachiocephalus myops	nd	nd	165±120	7.49±5.82	nd	9.44±8.20	18.4 ± 27.9	nd	201±98.6
Mollusk	*Turritella terebra bacillum*	nd	nd	nd	289±501	nd	nd	nd	nd	289±501
	Solen strictus	nd	nd	nd	14.3 ± 3.25	nd	nd	nd	nd	14.3 ± 3.25
	Meretrix meretrix	nd	nd	nd	326±190	nd	nd	nd	nd	326±190
	Loligo beka	nd	nd	19.8 ± 21.4	nd	nd	nd	nd	nd	19.8 ± 21.4
	Octopusocellatus	nd	nd	120±41.3	31.3 ± 42.2	nd	nd	nd	nd	152±83.2
Crustacean	*Penaeus penicillatus*	nd	nd	nd	nd	nd	nd	10.6 ± 10.0	nd	10.6 ± 10.0
	Parapenaeopsis hungerfordi	nd	nd	nd	nd	nd	nd	3.14±2.89	nd	3.14±2.89
	Metapenaeus affinis	nd	nd	110±191	nd	nd	nd	0.900 ±0.892	nd	111±190
	Oratosquilla oratoria	nd	nd	1625±904	nd	nd	107±126	nd	nd	1732±1002
Detection frequency in biota (%)		2.78	9.72	36.1	58.3	0.000	29.2	40.3	4.17	93.1

All the values are presented as the means ± standard deviations.
nd: all of the sample concentrations are lower than the MDL.
<MDL: the mean value is lower than the MDL.

TNBP, TEP, TCPP, TDCPP, and EHDPHP) and emerging OPFRs (T4tBPP and RDP) were not significantly related to TLs ($p > 0.05$, Figure S4).

Furthermore, we performed Monte Carlo simulations of the TMFs (TMF_{NPB}, $n = 10{,}000$) for all these OPFRs (Fig. 2 and S5). Bootstrap regression is frequently employed as a reliable supplementary method to OLS regression, as it is particularly suitable for the analysis of limited sample sizes and unequal samples. Among the E-OPFRs, the TMF_{NPB} of RDP was greater than 1, with probabilities of TMFs greater than 1 of 100 %. RDP has been found to have biomagnification potential in the food web of Poyang Lake, China, which is consistent with the results of this study (Yan et al., 2024). T4tBPP has a TMF_{NPB} of 1.21, with a 52.1 % probability of exceeding a value of 1, indicating moderate potential for biomagnification. In addition, iDDPHP has a TMF_{NPB} of 0.650 with a probability greater than 1 of 13.6 %, indicating its robust biodilution potential (Table S1). The TMF_{NPB} of the TPHP was 1.54, which is highly consistent with TMF_{OLS}. Significant biomagnification of TPHP has also been reported in the marine food webs of Laizhou Bay (Bekele et al., 2019), Pearl River Estury (Huang et al., 2023), and Liaodong Bay in China (He et al., 2023), suggesting its trophic transfer potential in the marine food web. The TMF_{NPB} values for legacy OPFRs (TEP, TCEP, TDCPP, TNBP and EHDPHP) were all >=1 in this food web, and the probabilities of observing TMFs > 1 were greater than 39.2 %. However, the TMF_{NPB} values for TCPP, TCP and TEHP were <1, and the probabilities of observing TMFs > 1 were <28.7 % (Table S2). A number of studies have reported the occurrence of trophic dilutions of TCP and TEHP in marine environments (Brandsma et al., 2015; He et al., 2023; Wang et al., 2023).

2.3. Partitioning and metabolic behavior of emerging and legacy OPFRs

In this study, we employed a fugacity-based approach to characterize the partition coefficients and mass distributions of legacy and emerging OPFRs in various biological phases accurately and assess their trophic transfer mechanisms in the estuarine food web. The pp-LFERs method allows for the normalization of contaminant concentrations in organisms to their mass fraction in each absorption phase. In general, the log $K_{lipid/water}$ values were greater than the log $K_{phospholipid/water}$ and log $K_{protein/water}$ values for OPFRs (Huang et al., 2023; Zhang et al., 2024).

Table 2
Details on the concentrations of 10 legacy OPFRs in seawater (ng/L, $n = 14$), sediment (ng/g dw, $n = 14$), and biological samples (ng/g lipid weight).

Categories	Species name	TEP	TCEP	TCPP	TDCPP	TPHP	TNBP	TBOEP	TCP	EHDPHP	TEHP	Σ_{10}L-OPFRs
Seawater	Dissolved phase	4.25 ±2.67	0.134 ±0.051	5.72 ±7.42	2.64±1.51	0.374 ±0.293	5.70 ±9.89	0.846 ±0.766	nd	9.33 ±6.21	0.570 ±0.403	29.6 ± 14.2
	Detection frequency (%)	100	100	71.4	92.9	100	100	100	0.000	100	100	100
	Particulate phase	0.530 ±0.324	0.001 ±0.002	0.625 ±0.391	0.217 ±0.286	0.054 ±0.030	0.021 ±0.030	0.032 ±0.034	0.148 ±0.307	13.4 ± 11.1	11.4 ± 8.67	26.4 ± 19.8
	Detection frequency (%)	100	7.14	100	71.4	100	78.6	92.9	57.1	100	100	100
	Total	4.78 ±2.76	0.135 ±0.051	6.34 ±7.63	2.86±1.61	0.428 ±0.312	5.72 ±9.91	0.878 ±0.776	0.148 ±0.307	22.7 ± 16.9	11.9 ± 8.82	55.9 ± 27.5
	Detection frequency (%)	100	100	100	100	100	100	100	57.1	100	100	100
Sediment		75.0 ± 60.8	0.014 ±0.006	5.91 ±3.99	17.9 ± 15.0	0.162 ±0.090	0.463 ±0.222	0.163 ±0.113	0.751 ±2.03	1.54 ±0.921	0.150 ±0.160	102±69.8
	Detection frequency (%)	100	100	100	100	100	100	100	57.1	100	78.6	100
Fish	*Epinephelus fasciatus*	44.1 ± 31.3	1.54 ±0.620	85.3 ± 86.5	210±203	126 ±60.4	74.0 ± 67.3	4721 ±2317	437 ±99.9	33.0 ± 11.6	22.5 ± 27.7	5755 ±2679
	Chorinemus formosanus	23.7 ± 10.4	0.267 ±0.287	nd	119±112	86.5 ± 119	5.51 ±3.31	1390 ±283	85.3 ± 89.0	1.26 ±2.18	12.5 ± 4.64	1724±238
	Acanthopagrus latus	6.01 ±3.75	0.113 ±0.035	6.54 ±6.09	26.1 ± 3.58	0.582 ±0.683	0.707 ±0.675	96.1 ± 166	nd	nd	0.652 ±0.072	137±168
	Terapon jarbua	59.1 ± 75.8	0.543 ±0.554	42.2 ± 50.9	167±257	29.0 ± 20.4	6.92 ±8.49	nd	nd	1.54 ±2.66	18.8 ± 27.8	325±441
	Siganus canaliculatus	0.962 ±1.67	0.474 ±0.527	nd	162±131	475 ±192	<MDL	nd	nd	nd	8.98 ±7.67	648±289
	Sillago sihama	19.4 ± 8.09	0.689 ±0.902	53.2 ± 51.0	96.9 ± 102	4.09 ±7.09	5.03 ±7.67	nd	5.01 ±8.68	nd	2.83 ±2.57	187±140
	Leiognathus brevirostris	49.7 ± 12.4	0.127 ±0.220	58.6 ± 49.8	nd	57.8 ± 24.0	nd	nd	nd	42.3 ± 21.8	7.98 ±13.8	217±59.9
	Pneumatophorus japonicus	13.3 ± 13.8	nd	0.748 ±1.30	95.1 ± 165	91.1 ± 51.1	13.1 ± 22.6	nd	nd	0.905 ±1.57	1.46 ±2.53	216±156
	Gnathanodon speciosus	3.29 ±3.60	0.414 ±0.380	59.4 ± 103	388±255	43.2 ± 37.3	11.9 ± 7.79	nd	50.5 ± 87.4	0.435 ±0.754	7.35 ±8.56	565±495
	Plectorhinchus	6.05 ±4.40	0.342 ±0.216	49.3 ± 85.3	21.0 ± 19.4	64.0 ± 39.6	2.57 ±1.08	nd	nd	<MDL	0.332 ±0.574	144±105
	Stolephorus chinensis	18.4 ± 0.910	1.15 ±0.568	nd	381±270	181 ±52.6	1.17 ±1.18	nd	46.6 ± 21.4	11.8 ± 9.30	6.46 ±4.62	648±345
	Trachinotus ovatus	44.9 ± 35.2	1.35 ±1.27	106 ±97.1	259±181	67.5 ± 48.1	27.3 ± 27.8	6.57 ±9.71	83.4 ± 123	36.0 ± 30.7	26.4 ± 23.7	658±488
	Pisodonophis boro	3.98 ±2.98	0.029 ±0.028	24.5 ± 39.2	184±200	7.71 ±6.72	0.966 ±1.67	0.035 ±0.060	19.3 ± 10.7	<MDL	2.39 ±2.25	243±262
	Lutjanus johni	0.738 ±1.28	0.091 ±0.091	7.93 ±7.31	37.2 ± 11.5	nd	1.35 ±2.17	nd	8.54 ±8.98	0.315 ±0.545	0.259 ±0.280	56.4 ± 15.6
	Trachiocephalus myops	nd	1.18 ±0.713	nd	26.4 ± 28.5	23.2 ± 6.67	8.88 ±11.3	nd	24.9 ± 21.9	12.1 ± 3.52	7.89 ±13.7	105±25.6
Mollusk	*Turritella terebra bacillum*	nd	1.96 ±1.29	414 ±217	76,328 ±13,968	25.6 ± 12.5	20.7 ± 6.84	nd	189 ±162	31.8 ± 35.4	81.2 ± 37.5	77,092 ±14,417
	Solen strictus	441 ±353	0.313 ±0.316	47.6 ± 82.4	50.9 ± 88.2	50.0 ± 17.6	nd	nd	466 ±373	28.6 ± 49.5	60.9 ± 53.0	1145±952
	Meretrix meretrix	216 ±193	0.212 ±0.106	33.2 ± 52.5	106±93.4	41.4 ± 2.59	nd	nd	313 ±271	297±259	414 ±209	1421±631
	Loligo beka	23.6 ± 20.7	0.296 ±0.165	2.97 ±5.15	141±38.4	21.4 ± 2.49	0.627 ±0.307	0.730 ±1.26	nd	0.251 ±0.316	9.85 ±17.1	201±42.9
	Octopusocellatus	61.0 ± 50.7	0.585 ±0.416	nd	nd	116 ±29.2	0.562 ±0.973	nd	82.8 ± 117	1.21 ±2.09	nd	262±136
Crustacean	*Penaeus penicillatus*	nd	1.77 ±0.564	373 ±48.0	26,850 ±883	2.77 ±0.728	14.2 ± 2.86	7.80 ±13.5	nd	0.662 ±1.15	7.33 ±12.7	27,258 ±920
	Parapenaeopsis hungerfordi	165 ±286	1.02 ±0.227	274 ±44.3	104,749 ±11,761	15.0 ± 10.9	0.163 ±0.283	nd	nd	nd	nd	105,205 ±11,780
	Metapenaeus affinis	192 ±225	2.10 ±0.250	211 ±74.3	37,264 ±30,019	45.8 ± 21.9	13.1 ± 9.34	1.17 ±2.03	285 ±359	25.1 ± 14.6	nd	38,039 ±30,159
	Oratosquilla oratoria	nd	1.43 ±0.878	307 ±218	14,242 ±23,084	122 ±118	11.1 ± 8.96	1.44 ±2.49	nd	40.4 ± 16.6	24.1 ± 41.7	14,750 ±23,370
Detection frequency in biota (%)		69.4	87.5	55.6	77.8	91.7	63.9	19.4	43.1	51.4	63.9	100

All the values are presented as the means ± standard deviations.
nd: all of the sample concentrations are lower than the MDL.
<MDL: the mean value is lower than the MDL.

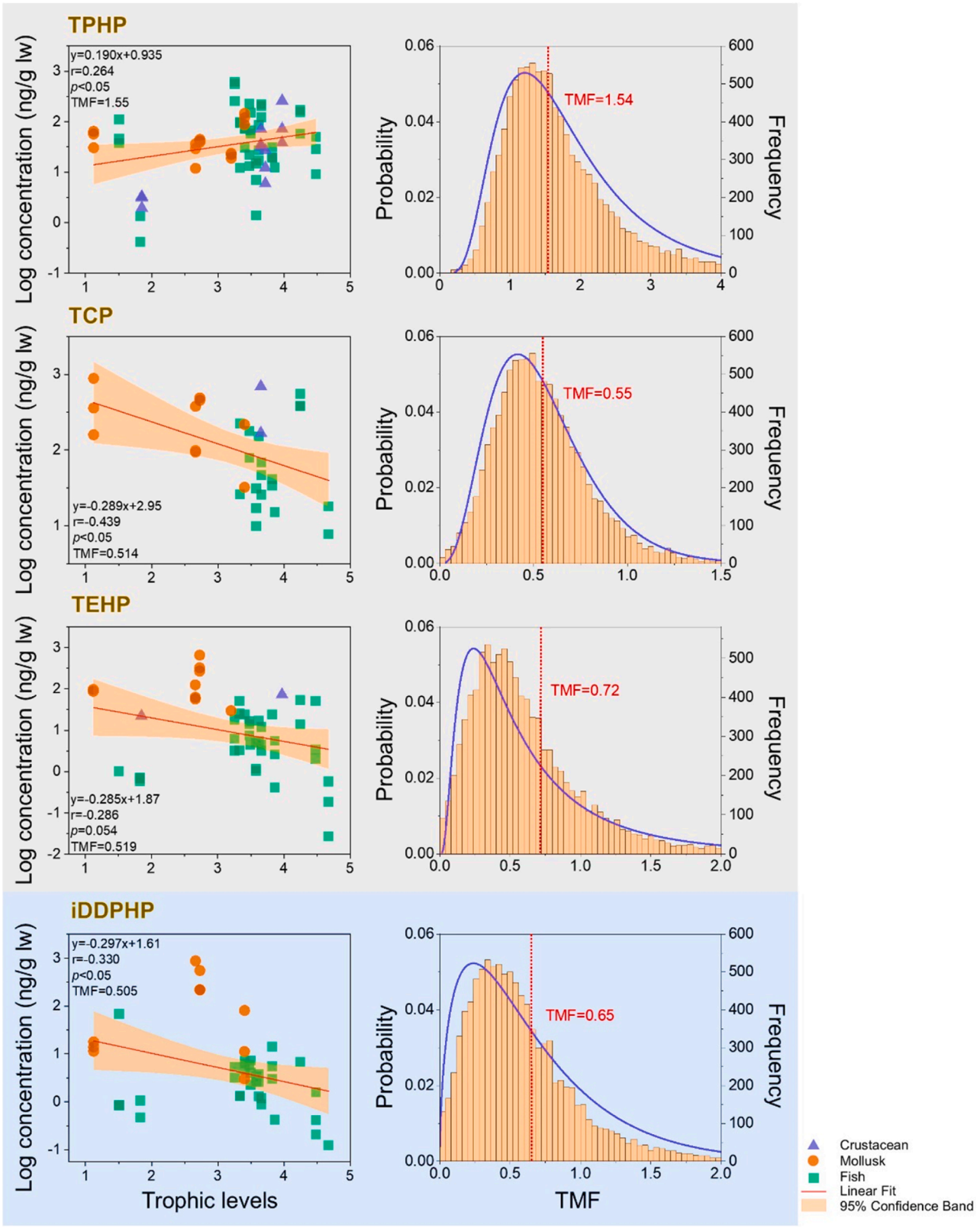

Fig. 2. Relationships between log-transformed concentrations of OPFRs (ng/g lw) and trophic levels (left side) and the frequency distributions of trophic magnification factors (TMFs) determined for lipid-normalized concentrations of OPFRs generated from bootstrapped Monte Carlo simulations (n = 10,000, right side) in estuarine food webs from Hainan Island, China.

Compared with legacy OPFRs, emerging OPFRs have relatively higher $K_{organism\text{-}water}$ values. The estimated $K_{organism\text{-}water}$ values were significantly correlated with Log K_{OW} for all the biota groups for OPFRs ($p < 0.01$, Fig. 3-A). These results confirmed the importance of hydrophobicity in the partitioning of OPFRs in marine organisms.

First, we found that the water content was the predominant absorption phase in all the biota samples (ranging from 66.6 % to 87.1 % of the mass), followed by structure protein (3.25–5.68 %), storage lipid (0.627–7.67 %) and phospholipids (0.120–0.200 %) (Figure S6). Considering that lipid, protein, phospholipid and water are important adsorption phases for the partitioning of organic pollutants, lipid-water/phospholipid-water/protein-water partition coefficients have been explored for their bioaccumulation/trophic magnification potential for emerging and legacy OPFRs (Droge, 2019; Fremlin et al., 2023). These results indicate that different trophic partitioning behaviors occurred for OPFR congeners in this food web. For TEP and TCEP, water content was the most important absorption phase for their mass distributions, and the mass distributions of storage lipid (29.1–85.4 %) and structural protein (13.2–65.9 %) were the two most important absorption phases for V6 (Fig. 3-B). The estimated mass fractions of the other 7 emerging OPFRs and 8 legacy OPFRs occurred mainly in storage lipid. Importantly, storage lipid did not significantly increase with increasing TLs ($r < 0$, $p = 0.591$; Figure S6), which may have resulted in an insignificant trophic transfer potential for most OPFRs in this study. Therefore, the variations in the absorption phase compositions may greatly control the partitioning of OPFRs in different food web members, which can also explain the different biomagnification conclusions for OPFRs across food webs (Borgå et al., 2012; Burkhard et al., 2013; Zhang et al., 2024).

A growing number of studies have indicated that the metabolism of OPFRs in organisms affects their bioavailability and limits their trophic transfer potential in food webs (Tang et al., 2019; Wang et al., 2019; Zhao et al., 2019). The total concentrations of the target OPFR metabolites increased in the following order: crustacean (30.7 ± 34.3 ng/g lw) < mollusk (49.5 ± 53.4 ng/g lw) < fish (50.6 ± 76.3 ng/g lw) ($p > 0.05$) (Table S4 and Figure S7-A). 4-hydroxyphenyl diphenyl phosphate (4-OH-TPHP) was the predominant OPFR metabolite, with a mean concentration of 27.5 ng/g lw, followed by di-n-butyl phosphate (DNBP), dibutyl-3-hydroxybutyl phosphate (3-OH-TNBP), and bis (2-butoxyethyl) phosphate (BBOEP) (Table S4 and Figure S7-B). The mass fraction of these OPFR metabolites in each absorption phase also did not show any positive correlations with the TLs (Figure S8). The significant relationships between TBOEP, TNBP and their corresponding metabolites suggest that there is a high probability that these two substances tend to be metabolized and accumulate in organisms (Figure S9). In the present study, we used the estimated K_M values via the EPA EPISuite BCFBAF™ for nonspecies-specific fish as a surrogate for the overall K_M of all OPFRs by various species in food webs (Table S5). The estimated K_M values of most legacy OPFRs were higher than those of emerging OPFRs (Fig. 3-A). It can be hypothesized that emerging OPFRs are inherently more difficult to metabolize in organisms and may accumulate more as parent compounds in the bodies of organisms.

2.4. Human dietary exposure and health risk assessment

In this study, we assessed the human health risks of target OPFRs and their metabolites via seafood consumption and used their concentrations in marine organisms to estimate daily intake (Fig. 4). HQ > 1 indicates a health risk for humans, whereas HQ < 1 indicates no risk. RfDs from references were adapted in this study and were calculated by applying the lowest NOAEL and reference maximum recommended composite uncertainty factors for the lowest reported NOAEL (Table S6). The HQs of all the OPFRs were in the range of 2.39×10^{-5}–7.93×10^{-2}. The relatively high HQs of TDCPP might be attributed to their relatively high exposure levels and low RfD. Generally, the total risk of human exposure to emerging OPFRs via seafood ingestion is relatively lower than that of legacy OPFRs. The bioavailability and permeability of compounds play key roles in the assessment of human exposure to OPFRs (Dahley et al., 2024; Pandey et al., 2024). Most legacy OPFRs have high gastrointestinal absorption according to an *in silico* tool (SwissADME; Table S7), indicating that emerging OPFRs may be relatively less bioavailable for humans. The probabilities of Caco-2 permeability were comparable between legacy and emerging OPFRs, but the aqueous solubilities of the emerging OPFRs, except for V6, were relatively lower (Log S < −4.0). This phenomenon may be attributed to the higher molecular mass of the emerging OPFRs. However, our study evaluated only OPFRs exposure via the dietary route, and the health risks of emerging OPFRs via multiple pathways should be assessed in the future. The high levels of some OPFR metabolites found in seafood cannot be ignored, which can provide valuable risk information for human exposure (Hou et al., 2023).

3. Conclusions

Understanding the partitioning and metabolism of OPFRs in marine organisms is far less understood but is key to assessing the trophic transfer potential of OPFRs in food webs. Although relatively high concentrations of the emerging OPFRs were detected in seawater and sediments from the investigated area, trophodynamic analysis revealed that the trophic transfer potential of the emerging OPFRs was lower than that of legacy OPFRs. Fugacity-based analysis indicated that different trophic partitioning behaviors occurred for the OPFR congeners in this food web. All the emerging OPFRs were found to be lipid-dominated in the organisms, but TEP and TCEP (the legacy OPFRs) showed significant water dominance in the food web members. Emerging OPFRs have relatively higher $K_{organism\text{-}water}$ values than legacy OPFRs do when accounting for the biological phase composition, but the relatively lower level of emerging OPFRs in the environment hinders their bioaccumulation and trophic transfer potential in the food web.

The consumption of seafood was found to present nonsignificant risks to local residents for both target legacy and emerging OPFRs. *In silico* bioavailability analysis also revealed a relatively lower gastrointestinal absorption potential of emerging OPFRs than legacy analogs. Nevertheless, it is advisable to maintain vigilance concerning the potential risks of emerging OPFRs from aquatic food webs, considering the gradual replacement of legacy OPFRs with emerging OPFRs in the future. Notably, we investigated only 8 metabolites of legacy OPFRs in this study. Comprehensive metabolite quantification of all OPFRs (especially E-OPFRs) can help characterize their bioaccumulation and trophodynamics in the food web.

4. Materials and methods

4.1. Chemicals and materials

The standards of 8 emerging OPFRs, including V6, CDP, RDP, iDDPHP, BDP, iPPP, T4tBPP and TDtBPP, and 10 legacy OPFRs, including TEP, TCEP, TCPP, TDCPP, TPHP, TNBP, TBOEP, TCP, EHDPHP and TEHP, were purchased with purities > 95 %. The 8 OPFR metabolites, including bis(2-butoxyethyl) hydroxyethyl phosphate (BBOEHEP), 3-OH-TNBP, 4-OH-TPHP, bis(2-butoxyethyl) 3-hydroxyl-2-butoxyethyl phosphate (3-OH-TBOEP), 2-ethyl-5-hydroxyhexyl diphenyl phosphate (5-OH-EHDPHP), diphenyl phosphate (DPHP), DNBP and BBOEP, were purchased with purities > 95 %. The detailed information of the abovementioned compounds is listed in Table S8. The isotope-labeled internal standard (IS) TNBP-d^{27} and surrogates for OPFRs (TPHP-d^{15}) and metabolites (BBOEP-d^{8}) were purchased from Toronto Research Chemicals (Toronto, ON, Canada). High-performance liquid chromatography-grade acetonitrile, dichloromethane, n-hexane, and methanol were purchased from OCEANPAK (Tianjin, China) or Merck (USA or Germany). The corresponding parent compounds for each of the metabolites are listed in Table S9.

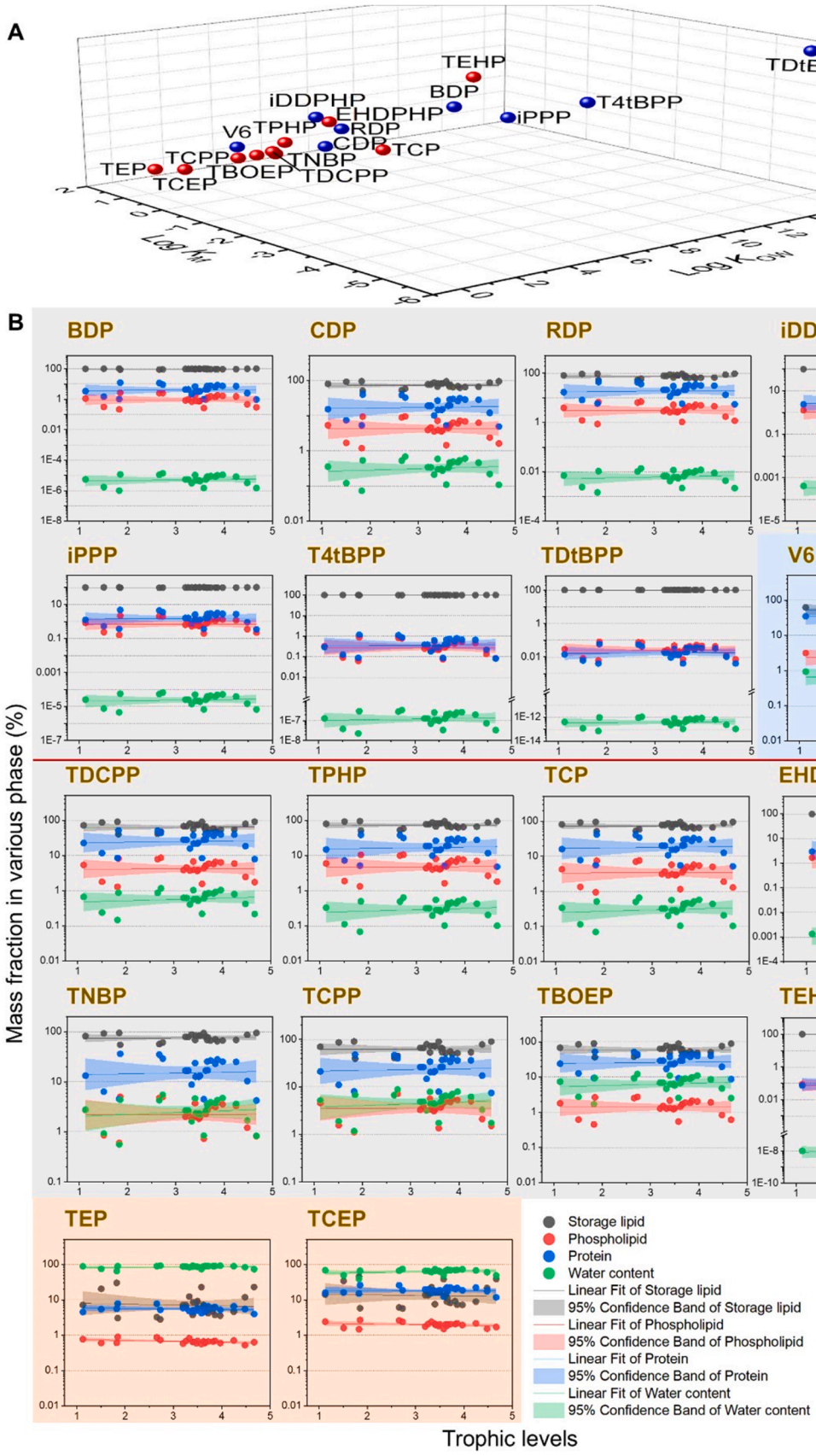

Fig. 3. (A) Estimated distributions of the Log $K_{organism\text{-}water}$ ratios of legacy OPFRs (red points) and emerging OPFRs (blue points) relative to Log K_{OW} and Log K_M. (B) Linear regressions between the mass fraction and TLs of 8 emerging and 10 legacy OPFRs.

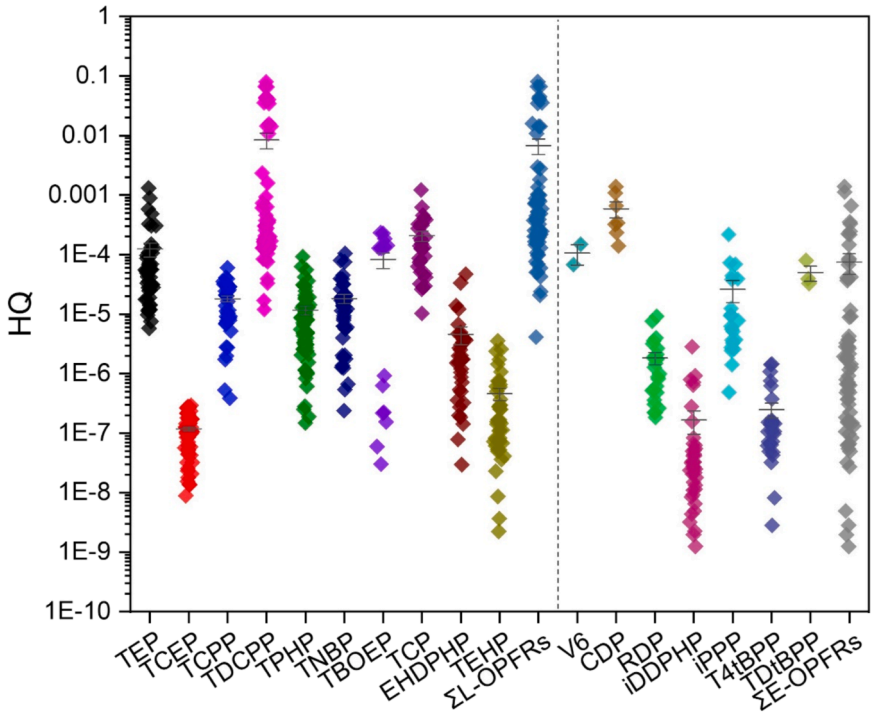

Fig. 4. Health risks of legacy and emerging OPFRs in seafood, measured in terms of hazard quotient (HQ).

4.2. Sampling sites and sample collection

All the environmental and faunal samples were collected from the Nandu River Estuary, China, in April 2023 (Figure S10). All the fauna samples were identified and classified on the basis of seafood databases (i.e., FishBase (https://www.fishbase.org), FishIDER (https://fishider.org/en), SeaLifeBase (https://www.sealifebase.org), and WoRMS (https://www.marinespecies.org)). The collected samples included fifteen fish species, including *Epinephelus fasciatus* (n = 3), *Chorinemus formosanus* (n = 3), *Acanthopagrus latus* (n = 3), *Terapon jarbua* (n = 3), *Siganus canaliculatus* (n = 3), *Sillago sihama* (n = 3), *Leiognathus brevirostris* (n = 3), *Pneumatophorus japonicus* (n = 3), *Gnathanodon speciosus* (n = 3), *Plectorhinchus* (n = 3), *Stolephorus chinensis* (n = 3), *Trachinotus ovatus* (n = 3), *Pisodonophis boro* (n = 3), *Lutjanus johni* (n = 1) and *Trachiocephalus myops* (n = 3). The five mollusk species included *Turritella terebra bacillum* (n = 3), *Solen strictus* (n = 3), *Meretrix meretrix* (n = 3), *Loligo beka* (n = 3) and *Octopusocellatus* (n = 3), and the four crustacean species included *Penaeus penicillatus* (n = 3), *Parapenaeopsis hungerfordi* (n = 3), *Metapenaeus affinis* (n = 3) and *Oratosquilla oratoria* (n = 3). Specifically, 54.1 % of these investigated species are carnivorous, 33.3 % are omnivorous, 4.17 % are deposit feeders, and 8.33 % are filter feeders. The majority of the species are benthic (62.5 %), with 33.3 % classified as coastal or pelagic and 4.17 % identified as coral reef fish. A detailed description of the collected organism samples is provided in Table S3. After collection, the samples were stored directly in a refrigerator at −20 °C and transported to the laboratory. Fourteen surface water samples and fourteen surface sediment samples were also collected in the sampling region.

4.3. Sample preparation and instrumental analysis

Detailed information on the preparation and treatment of the seawater, sediment and biota samples is provided in the Supporting Information (SI-1). Instrumental analysis of legacy and emerging OPFRs and metabolites was performed via Agilent 1290 Infinity ultra-high performance liquid chromatography coupled with Agilent 6470 triple quadrupole mass spectrometry (UPLC-MS/MS). The detailed UPLC and MS/MS parameters for the target analytes, surrogates, and IS are given in SI-2 and Table S10. The freeze-dried biota samples (0.5 mg) were used for analyzing stable isotopic ratios of carbon (δ^{13}C) and nitrogen (δ^{15}N) via a Flash EA 112 series elemental analyzer coupled with a Finnigan MAF ConFlo 111 isotope ratio mass spectrometer (Lu et al., 2023). The standard deviations for the δ^{13}C and δ^{15}N analyses were 0.02 % and 0.05 %, respectively. The water content of the biological samples was determined via the weighing method. The lipid content was determined gravimetrically using 0.1 g dw biological samples extracted with 1:1 v/v n-hexane and dichloromethane twice. Total protein and phospholipid levels in the biota samples were quantified via a Bicinchoninic Acid Assay Kit (Enzyme-linked Biotechnology Co., Shanghai, China) and a Phopholipid ELISA Kit (YJ218547, Yuanju Biotech, Shanghai, China), respectively.

4.4. Quality assurance and quality control (QA/QC)

All glassware was heated at 450 °C for 4 h before use, and all equipment (glassware, PTFE tube, etc.) was cleaned in sequence with methanol, dichloromethane, and n-hexane to decrease background interference. For each batch of samples (n = 12), a solvent blank, a method blank and a quality control (each target analyte at a concentration of 100 ng/mL) were run in sequence to check for carryover and system performance. Method blanks > 1 ng/mL were detected for TEP, TCPP, TDCPP, TPHP, and TDtBPP. The concentrations of the method blanks were subtracted from the corresponding samples. The surrogate recoveries for TPHP-d^{15} were 49.6–104 %, 65.4–85.0 %, and 53.4–138 % and those for BBOEP-d^{8} were 111–159 %, 85.4–123 % and 49.6–133 % for seawater, sediment and biological samples, respectively. The method detection limits (MDLs) and method quantitation limits (MQLs) were defined as the concentrations with signal-to-noise ratios of three and ten, respectively. The MDLs and MQLs of the target compounds ranged from 0.002 to 0.873 and 0.005–2.91 ng/g lw, respectively. The matrix effects for the target compounds ranged from 28.7 to 132 %. The utilization of matrix standards for the quantitative assessment of substances exhibiting high matrix effects. Spike recoveries were performed on the biological samples, with absolute recoveries ranging from 65.0 to

127 %. The intraday relative standard deviations (RSDs) were in the range of 0.957–22.0 %. Details of the QA/QC results for the seawater, sediment and biological samples are presented in Table S11.

4.5. Statistical analysis

The bioaccumulation factors (BAFs) are calculated to describe the transfer ratio of pollutants from water to biota via the following equations (Ma et al., 2014).

$$\mathrm{BAF}_{\mathrm{wet\ weight}} = C_{\mathrm{biota\ ww}} / C_{\mathrm{water}} \quad (1)$$

Where C_{water} is the sum of pollutant concentrations in the dissolved phase and particulate phase (ng/L) and C_{biota} is the concentration in biota (ng/g wet weight).

The biota-sediment accumulation factor (BSAF) is used to evaluate the bioavailability of pollutants from sediments and can be estimated via the following equation (Zhu et al., 2024):

$$\mathrm{BSAF} = C_{\mathrm{biota}} / C_{\mathrm{sediment}} \quad (2)$$

Where C_{biota} is the pollutant concentration in biota (ng/g wet weight) and C_{sediment} is the pollutant concentration in sediment (ng/g dry weight).

TLs of the analyzed organisms are estimated on the basis of the assumption that zooplankton occupy a TL of 2.0 and a $\Delta\sigma 15N$ of 3.4 via Eq. (3): (Yin et al., 2023)

$$TL_s = \left(\delta^{15}N_{\mathrm{samp}} - \delta^{15}N_{\mathrm{baseline}}\right) / \Delta\sigma^{15}N + \lambda \quad (3)$$

Where $\delta^{15}N_{\mathrm{samp}}$ and $\delta^{15}N_{\mathrm{baseline}}$ are the test $\delta^{15}N$ values of the biological sample and the baseline organism (zooplankton), respectively.

The calculation of TMFs is based on the correlations between lipid-normalized concentrations and the TLs of individual organisms via the following Eqs. (4)–(5):

$$\log\mathrm{OPFRs} = a + b{*}\mathrm{TLs} \quad (4)$$

$$\mathrm{TMFs} = 10^{b} \quad (5)$$

The partition coefficients for OPFRs and metabolites between the water and biological phases (i.e., lipid, protein and phospholipid) were estimated via the pp-LFERs method (SI-3 and Table S5). (Stenzel et al., 2013)

The relative fractions of the chemical mass of the target compounds (%) in each tissue phase can be estimated via Eq. (6): (Fremlin et al., 2023)

$$M_{tissue} = \frac{M_{tissue}}{M_{lipid} + M_{protein} + M_{phospholipid} + M_{water}} \times 100 \quad (6)$$

To evaluate the human health risk of OPFRs via seafood consumption, the estimated daily dietary intake (EDI) was calculated as follows: (Zhu et al., 2024)

$$EDI = C \times DC / BW \quad (7)$$

Where C is the concentration of the target compound in marine organisms (ng/g ww). DC represents the daily per capita seafood consumption of 82.4 g/person/day (Chen et al., 2023), and BW represents the average body weight of adults (70 kg) (Wang et al., 2020).

The health risk assessment via seafood consumption was evaluated (SI-4).

Univariate correlation analysis (Spearman correlation coefficients) was conducted to assess the concentrations between legacy and emerging OPFRs. All the statistical analyses were carried out via Origin 2022b software (Origin Lab Corporation, MA). A p value < 0.05, 0.01 or 0.001 was considered statistically significant. One-way analysis of variance (one-way ANOVA) was used to test the significance between groups, with a statistical significance level of 0.05. The chemical concentration below the MDLs was set to half of the MDLs for all the statistical analyses except linear regression.

CRediT authorship contribution statement

Qianyi Huang: Investigation, Data curation, Formal analysis, Visualization, Writing – original draft, Writing – review & editing. **Rui Hou:** Conceptualization, Investigation, Data curation, Writing – review & editing, Supervision, Funding acquisition. **Yuchen Wang:** Investigation, Data curation. **Lang Lin:** Investigation. **Hengxiang Li:** Investigation. **Shan Liu:** Investigation. **Xiangrong Xu:** Conceptualization, Investigation, Supervision, Project administration, Funding acquisition. **Kefu Yu:** Resources. **Xiaoping Huang:** Resources.

Declaration of competing interest

The authors declare that they have no known competing financial interests or personal relationships that could have appeared to influence the work reported in this paper.

Acknowledgments

This work was supported by the National Natural Science Foundation of China [No. 42277390], the Guangdong Basic and Applied Basic Research Foundation, China [No. 2024B1515020074], the Hainan Province Science and Technology Special Fund [No. ZDYF2022SHFZ317], and the Science and Technology Planning Project of Guangdong Province, China [No. 2023B1212060047].

Supplementary materials

Supplementary material associated with this article can be found, in the online version, at doi:10.1016/j.wroa.2024.100294.

Detailed information on the sampling, instrumental analysis, partition coefficient estimation and health risk assessment; tables showing the information on quality assurance and quality control results, biological parameters for individual samples, estimated partition coefficients, estimated bioaccumulation and biomagnification factors, acceptable daily intake values and human absorption parameters; figures showing sampling locations, bioaccumulation profiles of OPFR metabolites, relationships between legacy and emerging OPFR concentrations, relationships between log concentrations and trophic levels, relationships between metabolites and their parent OPFRs, frequency distributions of TMFs for some legacy and emerging OPFRs, and mass fractions of OPFR metabolites in the food web.

Data availability

The data that support the findings are available from the authors upon reasonable request.

References

China M.E.E., 2020. Priority chemicals list (second batch). https://www.mee.gov.cn/xxgk2018/xxgk/xxgk01/202011/t20201102_805937.html.

QYResearch, 2023. 2023–2029 Global and China Organophosphorus-based Flame Retardants Industry Research and 14th Five Year Plan Analysis Report.

Arnot, J.A., Gobas, F.A., 2006. A review of bioconcentration factor (BCF) and bioaccumulation factor (BAF) assessments for organic chemicals in aquatic organisms. Environ. Rev. 14 (4), 257–297.

Bekele, T.G., Zhao, H., Wang, Q., Chen, J., 2019. Bioaccumulation and trophic transfer of emerging organophosphate flame retardants in the marine food webs of Laizhou Bay, North China. Environ. Sci. Technol. 53 (22), 13417–13426.

Blum, A., Behl, M., Birnbaum, L.S., Diamond, M.L., Phillips, A., Singla, V., Sipes, N.S., Stapleton, H.M., Venier, M., 2019. Organophosphate ester flame retardants: are they a regrettable substitution for polybrominated diphenyl ethers? Environ. Sci. Technol. Lett. 6 (11), 638–649.

Borgå, K., Kidd, K.A., Muir, D.C., Berglund, O., Conder, J.M., Gobas, F.A., Kucklick, J., Malm, O., Powell, D.E., 2012. Trophic magnification factors: considerations of ecology, ecosystems, and study design. Integr. Environ. Assess. Manag. 8 (1), 64–84.

Brandsma, S.H., Leonards, P.E., Leslie, H.A., de Boer, J., 2015. Tracing organophosphorus and brominated flame retardants and plasticizers in an estuarine food web. Sci. Total Environ. 505, 22–31.
Burkhard, L.P., Borgå, K., Powell, D.E., Leonards, P., Muir, D.C.G., Parkerton, T.F., Woodburn, K.B., 2013. Improving the quality and scientific understanding of Trophic Magnification Factors (TMFs). Environ. Sci. Technol. 47 (3), 1186–1187.
Chen, X., Liang, X., Yang, J., Yuan, Y., Xiao, Q., Su, Z., Chen, Y., Lu, S., Wang, L., 2023. High-resolution mass spectrometry-based screening and dietary intake assessment of organophosphate esters in foodstuffs from South China. Sci. Total Environ. 905, 167169.
Choi, W., Lee, S., Lee, H.-K., Moon, H.-B., 2020. Organophosphate flame retardants and plasticizers in sediment and bivalves along the Korean coast: occurrence, geographical distribution, and a potential for bioaccumulation. Mar. Pollut. Bull. 156, 111275.
Dahley, C., Böckmann, T., Ebert, A., Goss, K.-U., 2024. Predicting the intrinsic membrane permeability of Caco-2/MDCK cells by the solubility-diffusion model. Eur. J. Pharm. Sci. 195, 106720.
Droge, S.T.J, 2019. Membrane–Water partition coefficients to aid risk assessment of perfluoroalkyl anions and alkyl sulfates. Environ. Sci. Technol. 53 (2), 760–770.
Du, J., Li, H., Xu, S., Zhou, Q., Jin, M., Tang, J., 2019. A review of organophosphorus flame retardants (OPFRs): occurrence, bioaccumulation, toxicity, and organism exposure. Environ. Sci. Pollut. Res. 26 (22), 22126–22136.
Endo, S., Goss, K.-U., 2014. Predicting partition coefficients of polyfluorinated and organosilicon compounds using Polyparameter Linear Free Energy Relationships (PP-LFERs). Environ. Sci. Technol. 48 (5), 2776–2784.
Fremlin, K.M., Elliott, J.E., Letcher, R.J., Harner, T., Gobas, F., 2023. Developing methods for assessing trophic magnification of perfluoroalkyl substances within an urban terrestrial avian food web. Environ. Sci. Technol. 57 (34), 12806–12818.
Fu, J., Fu, K., Chen, Y., Li, X., Ye, T., Gao, K., Pan, W., Zhang, A., Fu, J., 2021. Long-Range transport, trophic transfer, and ecological risks of organophosphate esters in remote areas. Environ. Sci. Technol. 55 (15), 10192–10209.
Gao, M., Zhang, Q., Wu, S., Wu, L., Cao, P., Zhang, Y., Rong, L., Fang, B., Yuan, C., Yao, Y., Wang, Y., Sun, H., 2024. Contamination status of novel organophosphate esters derived from organophosphite antioxidants in soil and the effects on soil bacterial communities. Environ. Sci. Technol. 58 (24), 10740–10751.
Geisler, A., Endo, S., Goss, K.-U., 2012. Partitioning of organic chemicals to storage lipids: elucidating the dependence on fatty acid composition and temperature. Environ. Sci. Technol. 46 (17), 9519–9524.
He, W., Ding, J., Liu, W., Zhong, W., Zhu, L., Zhu, L., Feng, J., 2023. Occurrence, bioaccumulation and trophic transfer of organophosphate esters in marine food webs: evidence from three bays in Bohai Sea, China. Sci. Total Environ. 861, 160658.
Hou, R., Sun, C., Zhang, S., Huang, Q., Liu, S., Lin, L., Li, H., Xu, X., 2023. The metabolism of novel flame retardants and the internal exposure and toxicity of their major metabolites in fauna - a review. J. Environ. Exposure Assess. 2 (2), 10.
Hou, R., Xu, Y., Wang, Z., 2016. Review of OPFRs in animals and humans: absorption, bioaccumulation, metabolism, and internal exposure research. Chemosphere 153, 78–90.
Huang, Q., Hou, R., Lin, L., Li, H., Liu, S., Cheng, Y., Xu, X., 2023. Bioaccumulation and trophic transfer of organophosphate flame retardants and their metabolites in the estuarine food web of the Pearl River, China. Environ. Sci. Technol. 57 (9), 3549–3561.
Kim, S.K., Lee, D.S., Oh, J.R., 2002. Characteristics of trophic transfer of polychlorinated biphenyls in marine organisms in Incheon North Harbor, Korea. Environ. Toxicol. Chem. 21 (4), 834–841.
Li, L., Chen, R., Wang, L., Jia, Y., Shen, X., Hu, J., 2023. Discovery of three organothiophosphate esters in river water using high-resolution mass spectrometry. Environ. Sci. Technol. 57 (18), 7254–7262.
Lian, M., Wang, J., Wang, Z., Lin, C., Gu, X., He, M., Liu, X., Wei, O., 2024. Occurrence, bioaccumulation and trophodynamics of organophosphate esters in the marine biota web of Laizhou Bay, Bohai Sea. J. Hazard. Mater. 469, 134035.
Liu, R., Mabury, S.A., 2018. Unexpectedly high concentrations of a newly identified organophosphate ester, tris(2,4-di-tert-butylphenyl) phosphate, in indoor dust from Canada. Environ. Sci. Technol. 52 (17), 9677–9683.
Lu, R., Cao, X., Zheng, X., Zeng, Y., Jiang, Y., Mai, B., 2023. Biomagnification and elimination effects of persistent organic pollutants in a typical wetland food web from South China. J. Hazard. Mater. 457, 131733.
Luo, W., Liu, Y., Yang, X., Aamir, M., Bai, X., Liu, W., 2023. Prenatal exposure to emerging and traditional organophosphate flame retardants: regional comparison, transplacental transfer, and birth outcomes. Environ. Pollut. 336, 122463.
Ma, X., Zhang, H., Wang, Z., Yao, Z., Chen, J., Chen, J., 2014. Bioaccumulation and trophic transfer of short chain chlorinated paraffins in a marine food web from Liaodong Bay, North China. Environ. Sci. Technol. 48 (10), 5964–5971.
Mo, L., Zheng, J., Wang, T., Shi, Y., Chen, B., Liu, B., Ma, Y., Li, M., Zhuo, L., Chen, S., 2019. Legacy and emerging contaminants in coastal surface sediments around Hainan Island in South China. Chemosphere 215, 133–141.
Pandey, N., Kumari, N., Roy, P., Mondal, S.K., Thakur, A., Sun, C.C., Ghosh, A., 2024. Tuning Caco-2 permeability by cocrystallization: insights from molecular dynamics simulation. Int. J. Pharm. 650, 123666.
Pantelaki, I., Voutsa, D., 2019. Organophosphate flame retardants (OPFRs): a review on analytical methods and occurrence in wastewater and aquatic environment. Sci. Total Environ. 649, 247–263.
Schang, G., Robaire, B., Hales, B.F., 2016. Organophosphate flame retardants act as endocrine-disrupting chemicals in MA-10 mouse tumor Leydig cells. Toxicol. Sci. 150 (2), 499–509.
Shi, H., Zhao, Y., 2024. Bringing the emerging organophosphate flame retardants (eOPFRs) into view: a hidden ecological and human health threat. Aquatic Toxicol. 267, 106833.
Stenzel, A., Goss, K.-U., Endo, S., 2013. Determination of Polyparameter Linear Free Energy Relationship (pp-LFER) substance descriptors for established and alternative flame retardants. Environ. Sci. Technol. 47 (3), 1399–1406.
Tang, B., Poma, G., Bastiaensen, M., Yin, S., Luo, X., Mai, B., Covaci, A., 2019. Bioconcentration and biotransformation of organophosphorus flame retardants (PFRs) in common carp (Cyprinus carpio). Environ. Int. 126, 512–522.
Tsugoshi, Y., Watanabe, Y., Tanikawa, Y., Inoue, C., Sugihara, K., Kojima, H., Kitamura, S., 2020. Inhibitory effects of organophosphate esters on carboxylesterase activity of rat liver microsomes. Chem. Biol. Interact. 327, 109148.
van der Veen, I., de Boer, J., 2012. Phosphorus flame retardants: properties, production, environmental occurrence, toxicity and analysis. Chemosphere 88 (10), 1119–1153.
Wang, H., Huang, W., Gong, Y., Chen, C., Zhang, T., Diao, X., 2020. Occurrence and potential health risks assessment of polycyclic aromatic hydrocarbons (PAHs) in different tissues of bivalves from Hainan Island, China. Food Chem. Toxicol. 136, 111108.
Wang, S., Zheng, N., Sun, S., Ji, Y., An, Q., Li, X., Li, Z., Zhang, W., 2023. Bioaccumulation of organophosphorus flame retardants in marine organisms in Liaodong Bay and their potential ecological risks based on species sensitivity distribution. Environ. Pollut. 317, 120812.
Wang, X., Zhong, W., Xiao, B., Liu, Q., Yang, L., Covaci, A., Zhu, L., 2019. Bioavailability and biomagnification of organophosphate esters in the food web of Taihu Lake, China: impacts of chemical properties and metabolism. Environ. Int. 125, 25–32.
Xie, Z., Zhang, X., Liu, F., Xie, Y., Sun, B., Wu, J., Wu, Y., 2024a. First determination of elevated levels of plastic additives in finless porpoises from the South China Sea. J. Hazard. Mater. 465, 133389.
Xie, Z., Zhang, X., Xie, Y., Liu, F., Sun, B., Liu, W., Wu, J., Wu, Y., 2024b. Bioaccumulation and potential endocrine disruption risk of legacy and emerging organophosphate esters in cetaceans from the Northern South China Sea. Environ. Sci. Technol. 58 (9), 4368–4380.
Yan, Z., Feng, C., Xu, Y., Wang, J., Huang, N., Jin, X., Wu, F., Bai, Y., 2024. Water temperature governs organophosphate ester dynamics in the aquatic food chain of Poyang Lake. Environ. Sci. Ecotechnol. 21, 100401.
Ye, L., Li, J., Gong, S., Herczegh, S.M., Zhang, Q., Letcher, R.J., Su, G., 2023. Established and emerging organophosphate esters (OPEs) and the expansion of an environmental contamination issue: a review and future directions. J. Hazard. Mater. 459, 132095.
Ye, L., Xing, L., Li, J., Kong, M., Su, G., 2022. Recognition of Organophosphate Esters (OPEs) in the sediment of 12 Lakes in the Taihu Lake Basin of China. ACS ES&T Water 2 (12), 2450–2459.
Yin, H., Chen, Y., Ma, W., Zhu, W., Wang, H., Zhou, Q., Li, J., Wang, A., Li, X., Xu, Q., 2023. δ13C and δ15N stable isotopes demonstrate seasonal changes in the food web of coral reefs at the Wuzhizhou Island of the South China sea. Ecol. Indic. 146, 109852.
Zhang, L., Yang, X., Low, W.V., Ma, J., Yan, C., Zhu, Z., Lu, L., Hou, R., 2024. Fugacity- and biotransformation-based mechanistic insights into the trophic transfer of organophosphate flame retardants in a subtropical coastal food web from the Northern Beibu Gulf of China. Water Res. 261, 122043.
Zhao, H., Liu, L., Li, Y., Zhao, F., Zhang, S., Mu, D., Liu, J., An, L., Wan, Y., Hu, J., 2019. Occurrence, bioaccumulation, and trophic transfer of oligomeric organophosphorus flame retardants in an aquatic environment. Environ. Sci. Technol. Lett. 6 (6), 323–328.
Zhou, R., Geng, J., Jiang, J., Shao, B., Lin, L., Mu, T., Wang, B., Liu, T., 2024. Contamination of dairy products with tris(2,4-di-tert-butylphenyl) phosphite and implications for human exposure. Food Chem. 448, 139144.
Zhu, R., Pan, C., Peng, F., Zhou, C., Hu, J., Yu, K., 2024. Parabens and their metabolite in a marine benthic-dominated food web from the Beibu gulf, South China Sea: occurrence, trophic transfer and health risk assessment. Water Res. 248, 120841.